Rapports internes du LaMSID

R. FERNANDES, C. CHAVANT

Evaluating the reliability of hydro-mechanical simulation : a benchmark of numerical techniques carried out by research group of MoMas

RI-B3-N°003 Novembre 2006

Laboratoire de Mécanique des Structures Industrielles Durables
UMR EDF-CNRS 2832
EDF R&D
1, Avenue du Général de Gaulle - 92141 CLAMART CEDEX FRANCE

Evaluating the reliability of hydro-mechanical simulation : a benchmark of numerical techniques carried out by research group of MoMas

Roméo Fernandes*, Clément Chavant

Laboratoire de Mécanique des Structures Industrielles Durables Unité Mixte de Recherche CNRS-EDF, UMR 2832, EDF/R&D, 1 avenue du Général de Gaulle, 92.141 Clamart Cedex, France

Abstract

The production of nuclear energy is today facing to the issue of the management of radioactive waste. A possible solution is mainly based on the storage of those wastes in deep geological formations. From a scientific point of view the main objective is the human protection as well as the environment to avoid any dissemination of those radioactive substance.

The research works aim to demonstrate the capability and the security of such solution. The approach consist in master the thermal, hydraulic, mechanic, and chemical perturbations induced by the storage. An important part of these research concerns the migration of the radionucleids through the environment and their return to the biosphere. The circulation of the groundwater is a potential vector of this dissemination.

Thus, the excavation of the underground works dedicated to the storage of the wastes produce the development of cracks and fractures in the rock that will modify the hydraulic properties of the soil creating then preferred zones for water flows. It appears essential to evaluate accurately the area of the zones damaged by the excavation work and their evolution during the time.

It is one of the mission given to the Research Group MoMas (Modélisation Mathématique et Simulations numériques) whose objective is to improve the numerical simulation tools for the analysis of feasibility and the evaluation of the safety of a potential storage of the nuclear wastes. It is in this context that the benchmark “simulation of an excavation within hydro-brittle mechanical behaviour” has been proposed.

The work presented here is the one carried out during the two last years. It highlights that the numerical simulation of the mechanical excavation of rocks under hydro-mechanical coupled conditions gives results depending on the spatial discretisation of the problem or on the numerical method if it has not been regularised. It is a well known issue in mechanic but it has never been evidenced in geomaterial mechanic with a hydraulic coupling.

---

* corresponding author : romeo.fernandes@edf.fr

Keywords : brittle fracture, permeability, coupling, localization.

Notation (constitutive equations):

p_w water pressure

ρ_w water volume mass

$\mathbf{M}_w$ water mass flow

S_w water saturation

φ porosity

K_w water incompressibility

k_w^{rel} relative water permeability

RH relative humidity

M_{ol} water molar mass

R ideal gas constant

T temperature

$k(\varphi)$ intrinsic permeability (dependence with porosity)

σ_{ij} total Cauchy stresses

σ'_{ij} effectives stresses

b Biot coefficient

s_{ij} deviatoric stresses

$s_{II}=\sqrt{s_{ij}.s_{ij}}$ norm of the deviatoric stresses

$I'_1=\delta_{ii}\sigma'_{ii}$ first stress invariant of effective stresses

γ^p equivalent deviatoric strain

$\varepsilon_v, \varepsilon_v^e, \varepsilon_v^p$ total, elastic and plastic volumetric strains

ε_{ij} total strains

$e_{ij}=dev(\varepsilon)_{ij}$

Notation (material properties):

$2\mu_0, 3K_0$ elasticity drained coefficient

E_0 drained Young modulus

ν_0 drained Poisson ratio

ϕ friction angle

c cohesion

γ_R^p ultimate value for equivalent deviatoric strain

Introduction and context

Radioactive waste management is an important environmental issue today. One of the possible solutions is the deep geological underground disposal. The main target of this solution is to build a geological barrier that will limit and delay the propagation of radionucleid in the biosphere. This propagation will be possible thanks to the groundwater flow. So it is essential to master the water flows from the stocking area.

The geological barrier is damaged during the excavation of the galleries dedicated to the storage of nuclear waste. The Excavation Damaged Zones (EDZ) will disturb the stability of the construction and alter the hydraulic properties of the soil. During the exploitation phase the EDZ will evolve because of the heat of the packages, of the water circulation and of the creep behaviour. Indeed, the cracking zones are characterised by an enhanced permeability, which leads to the creation of privileged ways for the water flows. We have to be able to predict, by calculation, the extent and the evolution of these EDZ under their mechanical and hydraulic aspects.

The modelling of theses coupled phenomena is still today a difficult issue. We have indeed to take into account the brittle aspect of the mechanical behaviour of the rock and the high raise of the permeability in the damaged area. We don't know how to demonstrate existence and unicity of the solutions of the corresponding non linear equations. Some analytical solutions exist for some tunnel excavation problems but under restrictive assumptions based on linear elastic laws of the soil or elastic perfectly plastic (Mestat 1999).

It is well known that the constitutive laws representing a material softening – like in rock mechanic – are initiating numerical instabilities. Darve (1995) shows that the solutions are depending on the type of finite elements, on their size and on their orientation. Lorentz (1999) shows that when the mesh is refined the energy dissipated to break the material tends to zero, which is physically not acceptable. So specific numerical treatment, regrouped under name of regularisation methods, has to be applied to these constitutive laws. Such methods exist and are widely used in the scope of mechanical simulation (see Francfort et Marigo (1993), Markov (1995), Frémond et Nedjar (1993), de Borst (1991), Pijaudier-Cabot (1995), Peerlings (1995), Chambon (2001), Lorentz (1999)). But to our knowledge those methods have never been applied to simulation coupled with hydraulic.

In this context, the Research Group MoMas proposed the benchmark "simulation of an excavation within hydro-brittle mechanical behaviour". The objective of this task is to evaluate if the numerical difficulties of the hydro-mechanical coupling are the same as the purely mechanical ones. In this perspective we propose to compare from a numerical point of view the results obtained by six participating teams. The issue deals with the simulation of an underground gallery excavation followed by a 10 years consolidation phase. One feature of this benchmark is the fact that all the equations, all the loadings, and all the boundary conditions are fixed. The participants are free to use any numerical resolution.

First of all we set all the equations of the hydro-mechanic coupled problem we assume to solve and we present all the numerical methods used by the teams. Then we show that when we use an elastic mechanic law perfectly plastic coupled with hydraulic the team's results are about the same (differences around 10%). Since the constitutive law becomes soft, we show that the results become sensitive to the numerical methods used and to the mesh discretisation. The benchmark required checking the impact of the boundary conditions on the behaviour of the water flow on the edge of the gallery. It appears that this choice is very important and has a big impact on the hydraulic results as well as on mechanical strength.

Definition and methodology for the benchmark

In this article, we are particularly interested in the numerical aspects. We would like to see if, as in the mechanical case, the use of the softening constitutive laws

with the hydraulic coupling problems creates results depending on the mesh or on the numerical methods. To be able to compare the team's results from an objective point of view it is necessary to specify similar equations, geometries and boundary conditions to the teams.

The choice of equations

We present hereafter the equations used in the benchmark to model the hydro-mechanical coupling behaviour of porous media. It is a brief introduction because this document purpose is not to present new equations. For more detailed information about the constitutive equations, the reader is invited to refer to Coussy (1995). The formulas that are not extracted from this book will be mentioned and explicitly referenced.

The test cases considered in the benchmark are from a hydraulic point of view, saturated with water (in most tests) or partly saturated with water and air (for one test). In the second case the desaturation happens only at the gallery border where the air pressure equal the atmosphere one. In these conditions the Richards assumption (Richards 1931) can be considered valid. By convention in this article, we suppose that the mechanical stresses are positive on traction, the deformations are positive on extension and the water pressure is positive on compression.

Starting with the hydraulic equations and considering S_w as the water saturation we express the water mass conservation with the relation:

$$\frac{\partial}{\partial t}(\rho_w \varphi S_w) + Div(\mathbf{M}_w) = 0 \quad (1)$$

The water constitutive equation expressed by Fernandez (1972) is:

$$\frac{d\rho_w}{\rho_w} = \frac{dp_w}{K_w} \quad (2)$$

The behaviour of the water flows is described by the classical formulation of the Darcy law for which we define a coupling between permeability and porosity $k(\varphi)$:

$$\mathbf{M}_w = -k(\varphi)\, k_w^{rel}(S_w)\, \nabla p_w \quad (3)$$

The equation of the porosity evolution is defined by:

$$\varphi - \varphi_0 = b\varepsilon_v + \frac{S_w(b-\varphi)}{K_s}\left(p_w - p_w^0\right) \qquad (4)$$

where the Biot coefficient b is assumed to be constant and the label 0 represent the initial conditions.

As described in the previous paragraph, a test case will take into account an environment partially saturated with water and air. We choose the Kelvin law to apply a relative humidity boundary condition:

$$\log(RH) = \frac{M_{ol}\left(-p_c\right)}{RT\ \rho_w} \qquad (5)$$

where $p_c = p_g - p_w$ is the capillary pressure and p_g is the gas pressure. The sorption curve considered for this case is a classical one of Van Genuchten type:

$$\begin{cases} if\ p_c > 0 & S_w(p_c) = \left(1 + \left(\frac{p_c}{A}\right)^{\frac{1}{1-B}}\right)^{-B} \\ if\ p_c \le 0 & S_w(p_c) = 1 \end{cases} \qquad (6)$$

where A, B are constants defined on Table 3. And the relative permeability formulation is defined by:

$$k_w^{rel}(S_w) = \left(1 + (S_w^{-2.429} - 1)^D\right)^{-1} \qquad (7)$$

where D is a constant defined on Table 3.

To introduce the coupling with the mechanics we consider the formulation written with effective stress according to the Bishop formalism (1963) in totally saturated conditions. In the partially saturated case various formulations exist where we can quote the Barcelone model in net stress (Alonso 1990), and the formulations from Modaressi (1994), Shrefler (1996), Dangla (1998). We will use the Dangla's method because the objective of this benchmark is not to compare the formulations:

$$\boldsymbol{\sigma} = \boldsymbol{\sigma}' - b\,\pi\,\mathbf{I} \qquad (8)$$

$$\text{with } \pi = (1 - S_w)\,p_g + S_w p_w - \frac{2}{3}\int_{Sw}^{1} p_c(\tau)\,d\tau \qquad (9)$$

In this benchmark we will consider two situations:

- Fully saturated situations for which particular form of (9) is: $\pi = p_w$ where we recover the Bishop formulation;

- Partly saturated cases with Richards's assumption (p_g=0) for which (9) is $\pi = S_w p_w + \frac{2}{3}\int_{Sw}^{1} p_w(\tau) d\tau$.

For mechanical equations we consider the momentum balance equation (under small deformations): $\mathbf{Div}(\sigma)+\rho\mathbf{g}=0$ (10)

To simulate the fracturation of the rock it is necessary to take into account a softening mechanical constitutive law. The literature provides many accurate constitutive laws for the rock mechanic. As our issue is numerical we prefer a simple law, easy to implement. For that reason, we chose an associated elasto-plasticity law with a Drucker-Prager model (Drucker and Prager (1952)). The elastic domain is defined from the effective stresses $\boldsymbol{\sigma}'$ by $F \leq 0$ with (see figure 1) :

$$F = \sqrt{\frac{3}{2}} s_{II} + \frac{2\sin\phi}{3-\sin\phi} I_1' - \frac{6c\, f(\gamma^p)\cos\phi}{3-\sin\phi} \qquad (11)$$

where $f(\gamma^p)$ reproduces the degradation of the material related to the deviatoric plastic strains :

$$\begin{cases} 0 < \gamma^p < \gamma_R^p & f(\gamma^p) = \left(1-(1-\alpha)\dfrac{\gamma^p}{\gamma_R^p}\right)^2 \\ \gamma^p \geq \gamma_R^p & f(\gamma^p) = \alpha^2 \end{cases} \qquad (12)$$

where α is a parameter to define the cohesion level (table 3). If $\gamma^p \geq \gamma_R^p$ we define the residual state of stress: $\sigma_{res} = \frac{6c\,\alpha^2\cos\phi}{3-\sin\phi}$.

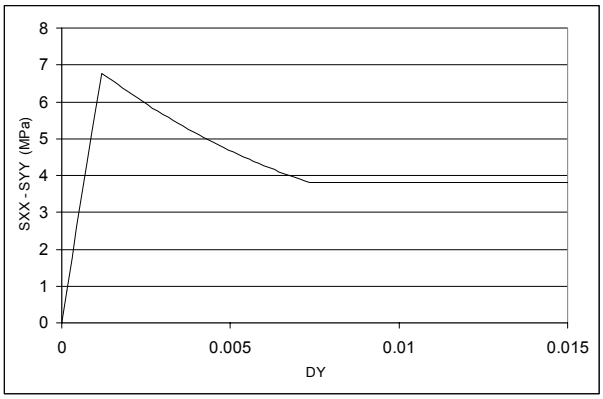

Figure 1. Triaxial stress state of Drucker-Prager law for a confinement of 2MPa.

The evolution of plastic strains is obtained by associated normal rule:

$$d\varepsilon_{ij}^{p} = d\lambda . \frac{\partial F}{\partial \sigma'_{ij}} \qquad (13)$$

And the effective stresses are related to total and plastic strains:

$$I'_1 = 3K_0(\varepsilon_v - \varepsilon_v^p) \qquad \text{and} \qquad s_{ij} = 2\mu_0 (e_{ij} - e_{ij}^p) \qquad (14)$$

With this formulation the local problem $\varepsilon \rightarrow (\sigma, \varepsilon^p)$ has only one solution.

To take into consideration the influence of the hydraulic behaviour we would like to take into account a coupling between permeability and damage. The damage is defined as the mechanical degradation of the material. To simplify, we consider in this benchmark that the damage is characterised by the plastic shear strain. Then, the increase of plastic shear strain produces the increase of plastic volumetric strain because argilite (material that is considered in the benchmark) is very dilating. Finally, considering the relation between the total, the elastic and the plastic volumetric strains $\varepsilon_v = \varepsilon_v^e + \varepsilon_v^p$ and noticing that the raise of the mechanical degradation induces $\varepsilon_v^p >> \varepsilon_v^e$, we can suppose that $\varepsilon_v \approx \varepsilon_v^p$. And taking into account the relation between porosity and total volumetric strain (eq. (4)), we assimilate in the benchmark the relation between permeability and damage to the following relation between permeability and porosity:

$$\frac{k(\varphi)}{k_0} = \begin{cases} 1 & \text{If} \quad \varphi - \varphi_0 < 0 \\ 1 + \chi(\varphi - \varphi_0)^3 & \text{If} \quad 0 < \varphi - \varphi_0 < 10^{-2} \\ 1 + 10^{-6}\chi & \text{If} \quad 10^{-2} < \varphi - \varphi_0 \end{cases} \qquad (15)$$

where the variable χ characterises the order of variation.

Numerical resolution

All the teams were free to use any numerical method and they all choose the finite element method. But the time and space discretisations of the hydro-mechanical coupling, the boundary conditions, the numerical integrations or the stopping criteria rely on the various methods chosen by the participants.

The teams participating are :

- The Grenoble laboratory L3S (Laboratoire Sols Solides Structures) in partnership with the mechanical institute of Liege University;
- The Lille laboratory LML (Laboratoire de Mécanique de Lille) ;
- The Nancy Laboratory Laego (Laboratoire environnement géomécanique et ouvrages) ;
- The LCPC of Paris (Laboratoire central des ponts et chaussées de Paris) ;
- The research centre of CEA (Commissariat de l'énergie atomique) ;
- The research centre of EDF (Electricité de France).

One of the differences noticed between the six teams comes from the continuous formulation expressed in large deformations by the L3S while the other participants consider small deformations.

Another difference between the participants is on the numerical integration of the hydro-mechanical coupling. The LCPC has indeed chosen an implicit discretisation partially coupled according to the relation (under water saturation):

$$\begin{cases} Div\,\boldsymbol{\sigma}\left(\mathbf{u}^{n+1},p^{n+1}\right)=0 \\ \dfrac{\rho_w^{n+1}\varphi^{n+1}-\rho_w^{n}\varphi^{n}}{t^{n+1}-t^{n}}-Div\left[\rho_w^{n}\dfrac{k_{\mathrm{int}}\left(\varphi^{n}\right)}{\mu_w}\nabla p^{n+1}\right]=0 \end{cases}$$

While the other teams used an implicit dicretisation totally coupled:

$$\begin{cases} Div\,\boldsymbol{\sigma}\left(\mathbf{u}^{n+1},p^{n+1}\right)=0 \\ \dfrac{\rho_w^{n+1}\varphi^{n+1}-\rho_w^{n}\varphi^{n}}{t^{n+1}-t^{n}}-Div\left[\rho_w^{n+1}\dfrac{k_{\mathrm{int}}\left(\varphi^{n+1}\right)}{\mu_w}\nabla p^{n+1}\right]=0 \end{cases}$$

Concerning the resolution of the global non linear problem the method everybody chose is the actualized Newton algorithm, except for CEA who use a pseudo-Newton method where the actualization of the tangent operator is not performed at each iterations.

On the other hand the Dirichlet type boundary conditions are set up by direct elimination method for L3S, LCPC and LML and by dualisation for the Laego, CEA and EDF. For the dripping boundary conditions EDF and CEA used the active set method while L3S used a penalization – the others did not participate to this study.

The finite element method leads to the numerical integration of polynomials which degree depends on the nodal variables interpolation. These variables are, in our coupled hydro-mechanical studies, the displacements and the water pressure. For the degrees of freedom interpolation the LML and LCPC define order 1 polynomials for the displacements and for the water pressure: it is P1P1 type interpolation. The geometrical discretisation of the considered domain is performed on linear elements for these two teams. The numerical integration being made by the Gauss quadrature for all the teams, we present in table 1 the finite elements and the number of integration points. Laego, CEA and EDF define polynomial interpolations P2P1 type (order 2 for displacements and order 1 for water pressure) while L3S used interpolations P2P2 type.

Teams	Interpolation type	Finite element for mechanic	Number of Gauss points for mechanic	Finite element for hydraulic	Number of Gauss points for hydraulic
L3S	P2P2	QU8	4	QU8	4
LCPC	P1P1	TR3	3	TR3	3
LML	P1P1	QU4	4	QU4	4
Laego	P2P1	TR6, QU8	3, 9	TR3, QU4	3, 9
CEA	P2P1	TR6, QU8	3, 8	TR3, QU4	3, 4
EDF	P2P1	TR6, QU8	3, 9	TR3, QU4	3, 9

Table 1 : Presentation of numerical integration formulations

The stopping criterion of the Newton algorithm is varying from one participant to another. Laego and EDF express this criterion with the relation: $\frac{\left\|\mathbf{R}\left(\mathbf{U}^{n+1}\right)\right\|_{\infty}}{\left\|\mathbf{L}-\mathbf{B}^{T}\Lambda^{n+1}\right\|_{\infty}}\leq\varepsilon$

where $\mathbf{L}$ is the external loading vector, $\mathbf{\Lambda}$ is the vector of Lagrange multipliers that dualize the kinematic relations (Bathe 1982), $\mathbf{B}^{T}\mathbf{\Lambda}$ represents the reaction forces, $\mathbf{R}\left(\mathbf{U}^{n+1}\right)$ is the residue of all the balance equations, and ε is the convergence criterion equal to 10^{-6}. A similar stopping criterion is used by CEA where the mechanical and hydraulic loadings are separate. The convergence criteria are set to 10^{-4} for the first and to 10^{-8} for the second. For L3S and LML

the stopping criterion is $\left\| \sqrt{\frac{\left(u_i^{n+1}-u_i^n\right)^2}{\left(u_i^{n+1}-u_i^0\right)^2}+\frac{\left(p^{n+1}-p^n\right)^2}{\left(p^{n+1}-p^0\right)^2}} \right\|_\infty \leq \varepsilon$ where the u is the displacement field and p the water pressure one. The convergence criterion ε is fixed to 10^{-6} by L3S and to 10^{-3} for the LML. The LCPC defines two stopping different criteria. The first one is on the mechanical part: $\frac{\|\Delta u_i\|_\infty}{u_{ref}} \leq \varepsilon$ and the second on the hydraulic part: $\frac{\|\Delta p_i\|_\infty}{p_{ref}} \leq \varepsilon$ where u_{ref} and p_{ref} are referenced values set to $10^{-3} m$ for the first and to $10^5 Pa$ for the second. The convergence criterion is set to 10^{-4}.

Finally, we find the last differences between the participants in the geometrical discretisation of the meshed surface (see table 2).

Teams	Number of nodes	
	1D cases	2D cases
L3S	353	2647
LCPC	101	1220
LML	402	861
Laego	244	2520
EDF	603	5776
CEA	423	1467

Table 2 : geometrical discretisation

The choice of study-cases

The main objective of the benchmark is to compare cases on dimension 2 with a softening mechanical law. But, before getting there, it is necessary to take simplest cases to check that the participants were consistent. For that, we considered one dimensional cases, bi-dimensional cases with perfectly plastic behaviour or with constant permeability.

In picture 2a, we present the geometry used for the 1D cases. The radius of cavity (R1) is 3 meters and the length (R2) for calculation domain is 20 meters. The initial conditions are isotropic conditions.

In picture 2b, we present the geometry used for the 2D cases. The radius of cavity is 3 meters and the horizontal and vertical length for calculation domain is 60 meters. We consider the following anisotropic initial conditions:

- $\sigma'_{xx} = -7.24 MPa$

- $\sigma'_{yy} = -11.64 MPa$
- $\sigma'_{zz} = -7.24 MPa$
- $p_w = 4.7 MPa$

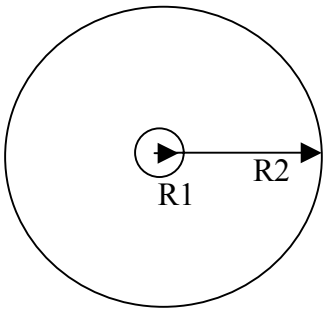

Figure 2a: 1D case

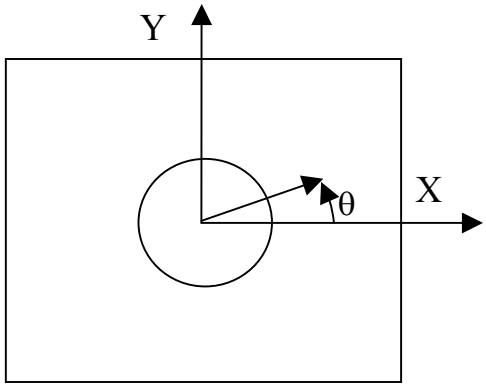

Figure 2b: 2D case

Figure 2 : Geometry for the test cases

The time of simulation is 17 days for excavation and 10 years for consolidation.

In the table 3, we defined the physical parameters values used for the benchmark and in the table 4, all the cases are resumed by their particular characteristics (dimension, mechanical behaviour, variation of permeability, hydraulic saturation condition,...). We describe more in detail those various parameters and more precisely their interest through the article.

Notations	**Parameters**	**values**
φ_0	Initial porosity	0.15
b	Biot coefficient	0.8
E_0	Drained Young modulus	5800 MPa
ν_0	Drained Poisson ratio	0.3
K_w	Water incompressibility	2000 MPa
k_0	Permeability	$10^{-12} m/s$
$\frac{k(\varphi)}{k_0}$: (15)	Permeability variation (2 possibilities)	χ=2.10^{-12} χ=2.10^{-10}
$S_w(p_c)$	Sorption curve (6)	A=10^7 B=0.412
k_w^{rel}	Relative permeability (7)	D=1.1760
c	Initial cohesion	1 Mpa
ϕ	Friction angle	25°

α	Parameter for (12) (2 possibilities)	0.01 0.5
γ_R^p	Ultimate value for equivalent deviatoric strain	0.015
ρ_w	Water volume mass	1000 kg/m3

Table 3. Physical parameters values.

Dimension	Mechanic Behaviour	Residual stress (Mpa)	Permeability	Hydraulic	Name
1D with isotropic initial state of stress	Softening	$\sigma_{res} \approx 0$	Constant	Saturated	Choice 6
	Softening	$\sigma_{res} = 0.53$	Variable	Saturated Dripping	Choice 7
	Softening	$\sigma_{res} = 0.53$	Variable	Unsaturated	Choice 8
2D with anisotropic initial state of stress	Perfectly plastic		Constant	Saturated	Choice 1
	Perfectly plastic		Variable	Saturated	Choice 2
	Softening	$\sigma_{res} = 0.53$	Variable	Unsaturated	Choice 3
	Softening	$\sigma_{res} \approx 0$	Constant	Saturated	Choice 4
	Softening	$\sigma_{res} = 0.53$	Variable	Saturated Dripping	Choice 5

Table 4. Particular characteristics of cases.

Analysis of the disparity between participants

One dimensional case

The results of the participants on the one-dimensional cases in isotropic initial conditions present no significant differences (around 1%). See curve (picture 3) representing the displacements on the studied axis after the simulation of a 10 years consolidation phase.

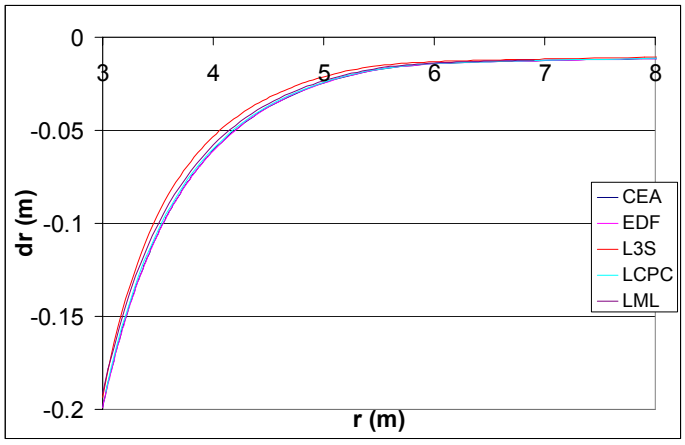

Figure 3 : radial displacements (10 years) on choice 6. Results of teams

Bi-dimensional case with an elastic perfectly plastic mechanical law

The comparative study of the 2D test cases with an elastic constitutive law perfectly plastic shows that the differences are growing but are still low. The displacements are close (see figure 4a) for the case – choice 1 - with constant permeability after a simulation of a 10 years period but we can notice that the differences happen on the effective stresses (lower than 10%, figure 4b).

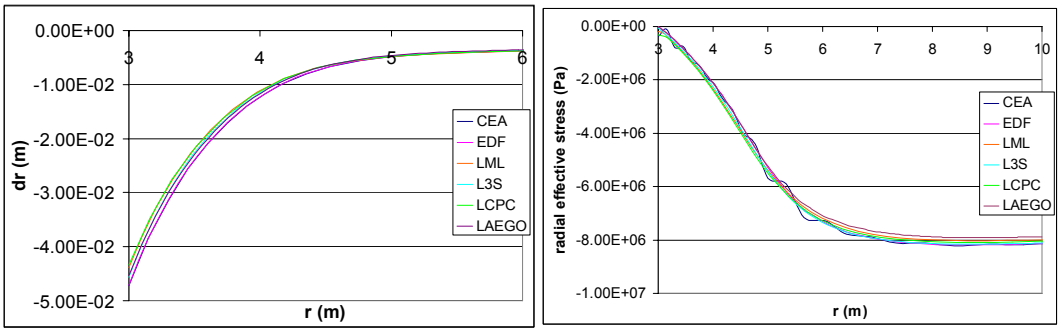

Figure 4a : Radial displacements Figure 4b : Radial effective stress

Figure 4 : Choice 1 (10 years). Results of teams

We suppose that those ones are coming from the lack of precision of the mesh in some teams. Indeed the space discretisations were very different from one participant to another: from 900 nodes for the coarsest one to 6000 for the finest (table 2). Creating a finest mesh we could reduce the differences.

Bi-dimensional case with a softening mechanical law

We consider now test cases with a softening mechanical behaviour and more particularly the case – choice 4 - for which the residual cohesion is near to 0. In order to evaluate the impact of the mesh discretisation on the results we suggested to use two meshes : a coarse one (M1) with the first level of elements around the gallery would have a lenght of 0.15 meters, and another one (M2) more precise with a ten times thinner mesh next to the gallery.

Comparing the results of participants at the end of the excavation (after 17 days) on the first mesh, we notice that the differences are not really significant. In fact, the disparity on the displacements (figure 5a) and on the plastic shear strains (figure 5b) stay small (lower than 15% between the participants).

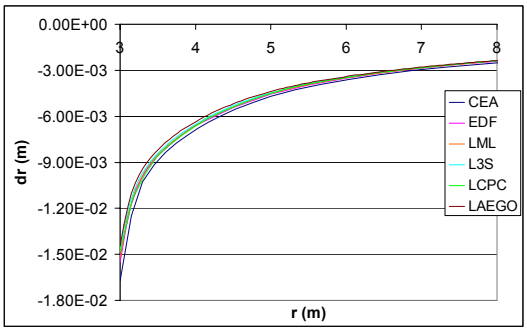

Figure 5a: radial displacements

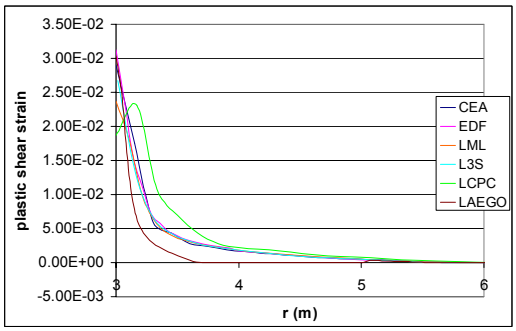

Figure 5b : plastic shear strain

Figure 5 : Choice 4 (17 days) with coarse mesh M1. Results of teams

If we now take into account the calculation with the second mesh, at the same time step, the results become very different. This is described on the picture 6 presenting the representative curves of the plastic shear strains obtained by EDF with the precise mesh face to the curves previously obtained with a coarse mesh. The only fact of changing the mesh has a short-term impact on the results.

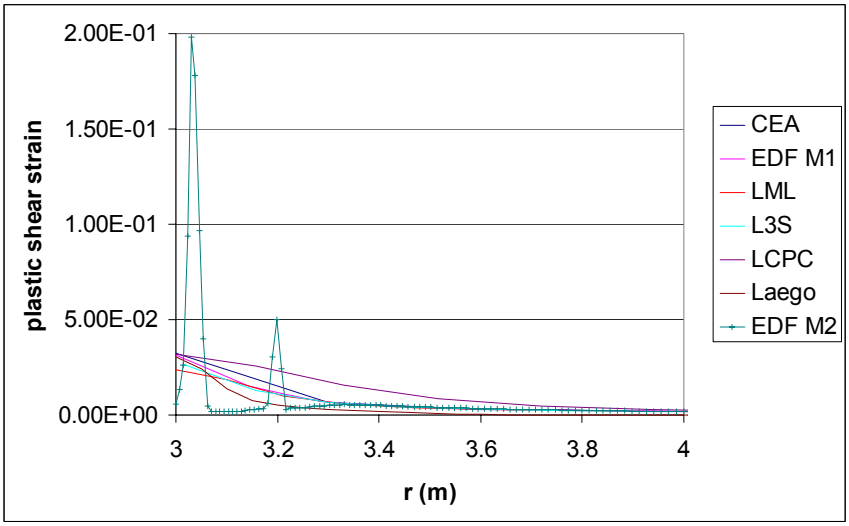

Figure 6: Choice 4 (17 days) with coarse mesh M1 and refined mesh M2. Plastic shear strain. Results of teams

The picture 7a and 7b show the isovalues of the plastic shear strains obtained by the L3S at 10 years using the two meshes. We notice that changing the mesh modifies the shear bandings.

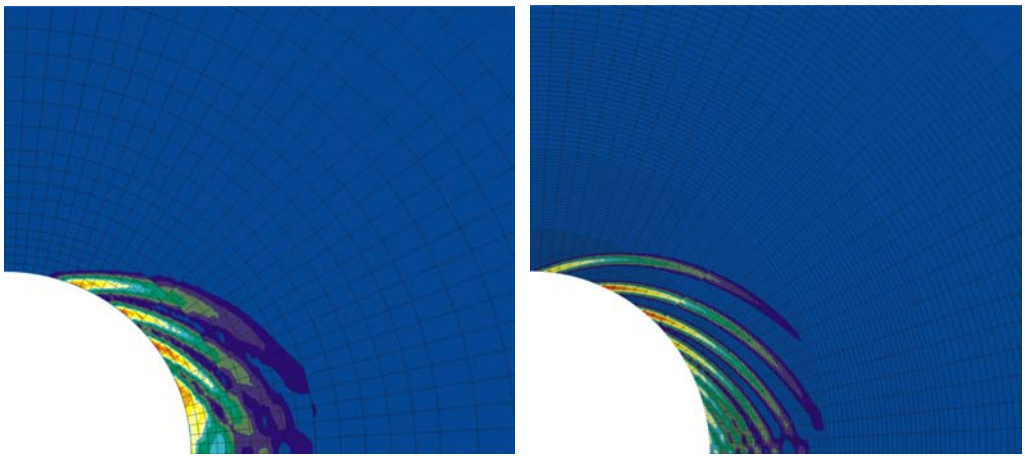

Figure 7. Choice 4. Geometric localisation of damaged zones.
a (at left) Coarse mesh M1. b (at right) Refined mesh M2

Following the calculation until 10 years on a coarse mesh and comparing the curves of plastic shear strains (picture 8), we observe a real disparity between participant's results (even if they're using equivalent meshes). Obviously, there is more than a single solution.

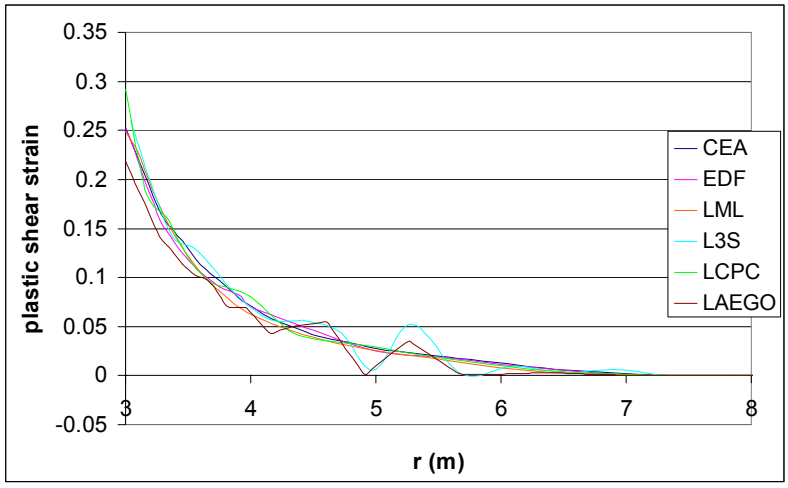

Figure 8: Choice 4 (10 years) with coarse mesh M1. Plastic shear strain. Results of teams

This fact can be studied looking at the influence of the initialisation of the Newton algorithm at each time step (see Matsushima and Chambon 2002). EDF and L3S are using two different strategies of Newton algorithm initialisation: for the first one the initial guess of the nodal variables is null while for the second the initialisation is obtained with an extrapolation from the previous time step according to the relation : $du_i^0 = \frac{\Delta t}{\Delta t^-} du_i^-$ where i is an index on the set of the nodal variable, exponent 0 representing the field initialisation and the indice '–'

representing the converged variables at a previous time step. We can observe on pictures 9a and 9b that, only after 17 days, the shear bands have different orientations. The results are strongly influenced by the numerical resolution.

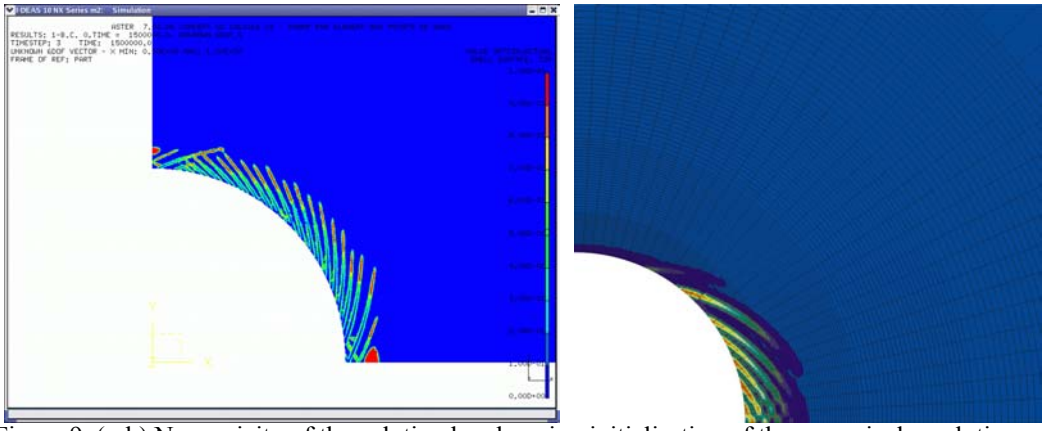

Figure 9. (a-b) Non-unicity of the solution by changing initialisation of the numerical resolution.

We highlight in this chapter that the use of a softening mechanical constitutive law in the coupled calculation with hydraulic provides results conditioned by the precision of the mesh or by the numerical methods like in the purely mechanic calculation. So we evidence the lack of reliability induced by the limitation of none regularised models.

Physical analysis of the study-cases and parameters influence

The benchmark enables to evaluate the impact of the various parameters on the results and on the numerical convergence of the calculation. These parameters have been selected because they correspond to values difficult to experimentally measure: permeability, hydraulic boundary conditions. So we present in the first part of this chapter a phenomenological analysis of the EDZ behaviour from 5 test cases. The main differences characterizing those tests are the variation of the permeability according to the rock damage, the softening or elastic perfectly plastic mechanical behavioural law, the dripping type hydraulic boundary conditions, the water pressure defined or the fixed hygrometry. In a second phase, we will propose an additional analyse on the numerical convergence of the calculation.

Physical analysis with respect to parameters variations

Each test case studied had been named in order to make the document easier to understand. So we will use the following terminology (see table 4 for precision):

- Choice 1: this case corresponds to the test in condition completely saturated with water, with an elastic perfectly plastic mechanical constitutive law and a constant permeability in the ground.
- Choice 2: this case is the same as the previous one except the permeability of the ground varies according to the rock damage.
- Choice 3: This case was defined to take into account the relative humidity at the gallery borders. We choose to set very high percentage of hygrometry (96%). This choice leads to a condition at the hydraulic limit up to a 5Mpa capillary pressure according to relation (5). We consider a simulation under the assumption of partial saturation with water and air. But in this case the saturation is still relatively high and close to one according to the sorption curve given by the relation (6). This case differs from the ohters because of the boundary conditions set. Moreover we use here the assumption of Richards (cf section 1.1) and we take into account the brittle aspect of the rock thanks to the softening mechanical law. And again the permeability varies according to the rock damage;
- Choice 4: It is a test in completely saturated condition, the mechanical constitutive law is soft and the permeability is supposed constant in all the ground. We set a null water pressure as a hydraulic boundary condition at the border of the gallery.
- Choice 5: This case was defined to study the impact of a dripping condition as a boundary condition. By dripping, we consider the

following unilateral condition: $p_w \leq p_0$; $\frac{\partial p_w}{\partial n} \geq 0$; $(p_w - p_0).\frac{\partial p_w}{\partial \mathbf{n}} = 0$.

This condition traduces the fact that water can go out of the field but can not go back. The test still remains under the condition of complete water saturation, the mechanical constitutive law is soft and the permeability varies according to the rock damage.

As showed in the previous chapter, the results obtained for the hydro-mechanic brittle type coupled studies are strongly linked to the mesh and to the numerical method. In order to compare the results of the five tests above from an objective point of view we will limit our observations to some studies made with the same software, with the same mesh (5800 nodes), with equivalent time steps (about 800 time steps for each test) and the same numerical method. The comparisons will be done on Y=0 axis for all the tests. We choose this axis because the initial state of stress $\left(\frac{\sigma_{xx}}{\sigma_{yy}} = \frac{\sigma_{zz}}{\sigma_{yy}} = 0.62 < 1 \right)$ leads to maximal shear on this axis.

Comparing the water pressure (figure 10a) and the displacements (figure 10b) at the end of the excavation, we notice the curves associated to the softening laws have common properties. Indeed we notice the appearance of a succion pressure in the first meter from the gallery border of the same range for the three tests and the displacements stay low (around centimetres). This phenomenon is explained at short term by the influence of the dilatance in the material considered. Under deviatoric strain the rock is damaging and its volume increases. This phenomenon happens during excavation work. The volume increase induces an increase of the environment porosity (cf. eq. 4) and as the rock is very impermeable material – the water circulation in is very low – the water pressure is lowering and can become negative creating the succion phenomena. The assumption of the effective stresses of Bishop implies a water pressure reduction and moreover a negative pressure equivalent to an improvement of the material cohesion. The modelling used in the benchmark probably over estimate this phenomenon even if it has already been experimentally observed. Mokni and Desrue (1999) demonstrated that the « non drainage can preclude localisation as long as cavitation in the pore-fluid does not relax the isochoric constraint ».

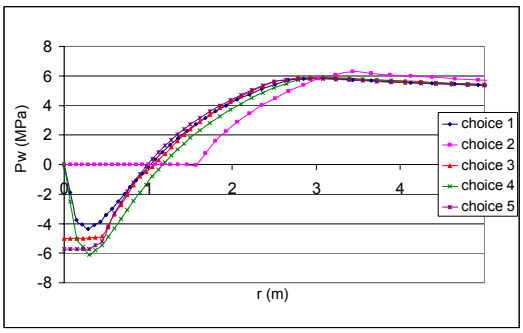

Figure 10a: water pressure

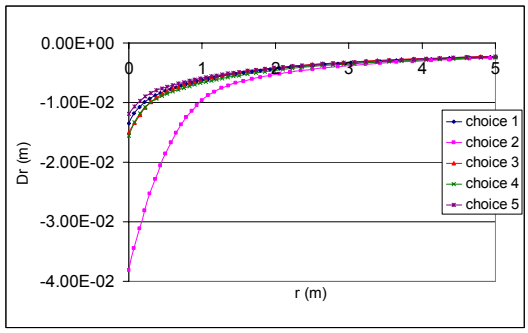

Figure 10b : radial displacements

Figure 10: Influence of parameters. Comparison after 17 days.

Finally we notice that when the permeability is defined as a function of the rock damage a constant water pressure level appears from the gallery borders until the first metre of the ground. The curves of the tests choice 2, 3 and 5 show this phenomenon (figure 10a). When the hydraulic boundary condition is a water pressure equal to zero, there is no negative pressure and the material behaviour is close to the one with drained conditions. Then the displacements at the end of the excavation are more important even if the mechanical law is elastic perfectly plastic as we can notice on the curve of choice 2 (figure 10b).

After 10 years consolidation, we notice picture 11a that the succion level stays unchanged in the non-saturated case. We notice that maintaining the 5Mpa capillary pressure at the gallery border is really different from the dripping condition. In the dripping case the level of water pressure at the gallery border rise again with the time; maintaining the 5Mpa pressure in the choice 3 stops the development of any phenomena (displacement, stresses, plastification).

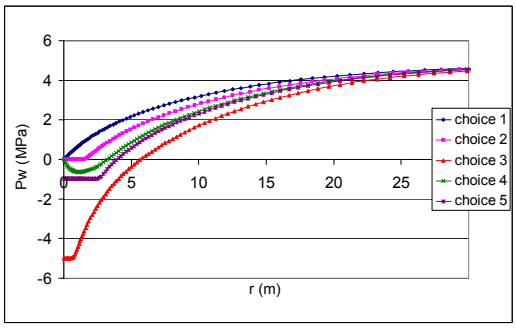

Figure 11a: water pressure

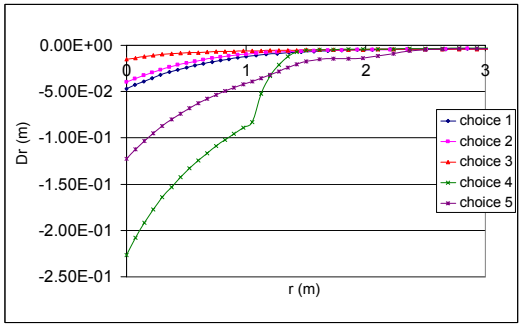

Figure 11b : radial displacements

Figure 11: Influence of parameters. Comparison after 10 years.

On the other hand, for the other cases with a softening behaviour – choice 4 and choice 5 -, the level of the water pressure clearly increased and the succion

phenomena has nearly disappeared. This process is explained by the material breaking at long term which improves the water circulation in the fractured zones. The rise of the water pressure is equivalent to the reduction of rock cohesion and this process will continue to develop. This phenomenon is confirmed by the results obtained picture 11b representing the displacement variation during the consolidation phase. We obtain an increase of the displacements at the borders of the gallery around 10 cm for test choice 5 – within dripping conditions – and more than 20 cm on test choice 4 – null water pressure.

At longer term we show that the choice of the hydraulic boundary conditions are important for the hydraulic results but as well on the mechanical strength of the work. Indeed, we notice the dripping boundary condition enables to reduce the displacements at the borders of the gallery despite taking into account the variation of permeability according to the rock damage. The test with the water pressure set to zero at the gallery border is still the one producing the most important mechanical displacement even if the permeability is supposed constant in the entire environment independently of the damaged zones.

Numerical analysis

From a numerical point of view we notice that all the teams had problem to perform the simulation of the choice 4. In the previous part we made the parameters vary to analyse their impact in the physics. We will now make these parameters vary to identify their impact on the numerical convergence and on the calculation. The parameters we consider are the permeability according to the rock damage, the scale of this variation, and the dripping condition. Theses ones lead to the definition of 4 new cases (table 5).

We begin to define a reference case – case 1 – presented in the table 5. This test is characterized by a permeability varying in an important matter according to the rock damage (6 scales following the definition of the relation 15), a residual cohesion equal to zero and a pressure equal to zero set to the gallery border. All the studies presented in this part are from a phenomenological point of view identical to the benchmark ones – excavation realised in 17 days followed in a 10 years consolidation phase – from a numerical point of view all realised with the same equivalent space discretisation, the same software, an equivalent time discretisation and the same resolution method. Only one parameter will be

modified at each time according to the reference case 1 and the convergence are presented in table 5.

	Case 1	Case 2	Case 3	Case 4
Properties	6 orders of variation for permeability $\sigma_{res} \approx 0MPa$	6 orders of variation for permeability $\sigma_{res} \approx 0MPa$ dripping	6 orders of variation for permeability $\sigma_{res} = 0.53MPa$	4 orders of variation for permeability $\sigma_{res} \approx 0MPa$
Excavation	28.6 cm	1.04 cm	9.84 cm	21.3 cm
Consolidation	No numerical convergence	8.23 cm	10.79 cm	No numerical convergence

Table 5. Analysis of the influence of parameters. Displacements and numerical convergence

This reference test is deliberately defined by a very severe coupled behaviour. Indeed as we already showed in the previous part the evolution of the permeability in the damaged zones will accelerate the collapse of the material. So we notice at the end of the excavation the maximal displacement of the gallery border is about 28.6 cm and the consolidation phase can't be reached because of non-convergence of the Newton algorithm.

We obtain the case 2 by modifying the hydraulic condition at the gallery border with a dripping condition. The numerical impact of this modification is noticeable. At the end of the excavation the gallery deformation is only around 1cm and the consolidation phase is numerically reached at the end of the 10 years simulation. Dripping is clearly a significant parameter. However, we notice after ten years the displacement reaches more than 7cm. So the very positive numerical influence of the dripping condition might vanish on the long term.

By increasing the parameters characterising the residual cohesion according to case 1 – then we obtain case 3 - we decrease the displacement at the end of the excavation (to 10 cm), but with a lower speed than through the dripping condition. But during the consolidation phase the deformation has increased less than a centimetre. This parameter is also significant but with a longer extent than the dripping condition.

The magnitude of the permeability variation has an influence on the hydro-mechanical behaviour but doesn't seem to be an important variable from a

numerical point of view. In fact, reducing of 2 scales the variation of maximal magnitude of the permeability according to the damage (going from 6 to 4 scales) – case 4 - the deformation at the gallery border at the end of the excavation has been reduced but is still high. The calculation cannot achieve the simulation of the consolidation phase because of non-convergence of the Newton algorithm like for the case 1.

Conclusions

We highlight, in this benchmark, that the simulation of coupled phenomena involving a softening mechanical law and hydraulic flows give numerical results strongly depending on the mesh discretisation or on the numerical method. This result is the same than for uncoupled mechanical simulation. Hydraulic flows induce no regularisation. From this point of view we estimate the results not reliable and it is necessary to continue the research work to define regularisation methods in order to accurately simulate the hydraulic behaviour produced by the degradation of the environment.

We also evidence that the hydraulic flow highly impacts the mechanical strength of the work. We tested three possible cases of hydraulic boundary conditions, and demonstrated that the mechanical strength is highly dependent of these conditions. Research work is still needed in this area in order to better understand these boundary conditions.

Reference

Abou-Bekr N., 1995. "Modélisation du comportement mécanique et hydraulique des sols partiellement saturés". Thèse ECP, France.

Alonso EE., Gens A., Josa A., 1990. "A constitutive model for partially saturated soils". Géotechnique 40, n°3, pp 405-430.

Bathe KJ., 1982. "Finite Element Procedures in Engineering Analysis". Prentice-Hall : Englewood Cliffs, NJ. 110-111, 182-185.

Bishop AW, Blight GE, 1963. Some Aspects of Effective Stress in Saturated and Partly Saturated Soils, *Geotechnique* n°3 vol. XIII : 177-197.

Bossat P., Meier PM., Moeri A., Trick T., Mayor JC, 2002. "Geological and hydraulic characterisation of the excavation disturbed zone in the Opalinus Clay of the Mont Terri Rock Laboratory", Engineering Geology, n°66, 19-38.

Chambon R., Caillerie D., Matsushima T., 2001. "Plastic continuum with microstructure, local second gradient theories for geomaterials : localization studies". International Journal of Solids and Structures, vol 38, pp. 8503-8527.

Chambon R., Collin F., 2004. "Hydromechanical numerical modeling of geotechnical problems using local second gradient models". Modelling of Cohesive Frictional Materials Vermeer Ehlers Hermann Ramm eds. AA Balkema : 209-221.

Chambon R., Crochepeyre S., Charlier R., 2001. "An algorithm and a method to search bifurcation points in non linear problems". International Journal for Numerical Methods in Engineering vol. 51, 315-332.

Chavant C., Debruyne G., Granet S., Sellali N., 2002. "*Numerical modeling of nuclear waste disposal*", 6th KIWIR, Paris.
Coussy O., 1995. *Mechanics of Porous Continua*, John Wiley&Sons.
Dangla P., Coussy O., 1998. "Non-linear poroelasticity for unsaturated porous materials : an energy approach". Poromechanics, A tribute to M.A. Biot, Proceedings of the Biot conference on poromechanics, Thimus J-F et al (dir.), Balkema, Rotterdam.
Darve F., Hicher PY., Reynouard JM., 1995. "Mécanique des géomatériaux" Hermès, Paris pp 103-121.
De Borst R., 1991. "Simulation of strain localization : a reappraisal of the Cosserat continuum". Eng. Comp., 8, pp. 317-332.
Drucker DC., Prager W., 1952. "Soil mechanics and plastic analysis design". Quaterly Journal of Applied Mathematics, vol 10, pp. 157-165.
Fernandez RT., 1972. "Natural convection from cylinders burried in porous media". PhD Thesis. University of California.
Francfort G., Marigo JJ, 1993. "Stable damage evolution in a brittle continuous medium". Eur. J. Mech. A/Solids, 12, no 2, pp. 149-189.
Frémond M., Nedjar B., 1993. "Endommagement et principe des puissances virtuelles". CRAS, t 317, série II, pp. 857-864.
Kolmayer Ph., Fernandes R., Chavant C., 2004. "Numerical implementation of a new rheological law for argilites", Applied Clay Science 26, 499-510.
Lewis RW, Schrefler BA, 1998. "The finite element method in the static and dynamic deformation and consolidation of porous media". Wiley.
Lorentz E., 1999. "Lois de comportement à gradients de variables internes : construction, formulation variationnelle et mise en oeuvre numérique". Thèse de doctorat de l'Université Paris 6.
Markov K., 1995. "On a microstructural model of damage in solids". Int. J. Eng. Sci. 33, no 1, pp. 139-150.
Matsushima T. Chambon R., Caillerie D., 2002. « Large strain finite element analysis of a local second gradient model : application to localization » Int. J. Numer. Meth. Engng; 54 : 499-521.
Mestat Ph., 1993. "Loi de comportement des géomatériaux et modélisation par la méthode des éléments finis", Presses du LCPC, série géotechnique GT52.
Mestat Ph., Prat M., 1999. "Ouvrages en interaction". Hermes Science Publications, Paris.
Modaressi A., Abou-Bekr N., 1994. "A unified approach to model the behavior of saturated and unsaturated soils", Computer Methods and Advances in Geomechanics, Proceedings of the Eighth International Conference on Computer Methods and Advances in Geomechanics. H.J. Siriwardane and M.M. Zaman (ed.), Balkema, 1507-1513.
Mokni M., Desrues J., 1999. "Strain localization measurements in undrained plane-strain biaxial tests on Hostun RF sand". Mechanics of cohesive frictional materials, 4, pp 419-441.
Peerlings RHJ., de Borst R., Brekelmans WAM., de Vree JHP., 1995. "Computational modelling of gradient-enhanced damage for fracture and fatigue problems". In proceedings Computational Plasticity IV, Owen & Oñate eds, pp. 975-986.
Pijaudier-Cabot G., 1995. "Nonlocal damage". In Continuum models for materials with microstructures, HB Mühlhaus ed., Wiley.
Richards LA, 1931. "Capillary conduction of liquids through porous mediums". Physics 1, 318-333.
Schrefler BA., Sanavia L., Majorana CE., 1996. "A multiphase medium model for localisation and postlocalisation simulation in geomaterials". Mechanics of cohesive-frictional materials. Vol 1, pp 95-114.